Available online at www.sciencedirect.com
SCIENCE DIRECT®
Journal of Magnetic Resonance 171 (2004) 186–191
JMR Journal of Magnetic Resonance
www.elsevier.com/locate/jmr

The DQ-HN{CACB} and DQ-HN(CO){CACB} sequences with evolution of double quantum C_α–C_β coherences

Wiktor Koźmiński[a,*], Igor Zhukov[b]

[a] Department of Chemistry, Warsaw University, ul. Pasteura 1, 02-093 Warszawa, Poland
[b] Institute of Biochemistry and Biophysics, Polish Academy of Sciences, ul. Pawińskiego 5a, 02-106 Warszawa, Poland

Received 25 June 2004; revised 19 August 2004
Available online 22 September 2004

Abstract

The new variant of known HNCACB and HN(CO)CACB techniques is proposed that employs excitation and evolution of double quantum C_α–C_β coherences. The most important features of the new method are: increased signal dispersion, lack of splittings due to $^1J(C_\alpha–C_\beta)$ spin–spin couplings, and absence of accidental cancellations of positive and negative signals. The acquisition of both DQ-HN{CACB} and DQ-HN(CO){CACB} techniques enables sequential assignment of protein backbone, using only C_α–C_β DQ-frequencies. The determination of all C_α and C_β chemical shifts requires, however, a comparison with HN(CO)CA or HNCA spectra. Examples of applications of the DQ-HN{CACB} and DQ-HN(CO){CACB} experiments are presented, employing the 2D Reduced Dimensionality approach for ^{13}C, ^{15}N-labeled ubiquitin, and the 3D acquisition for ^{13}C, ^{15}N-double labeled Ca^{2+}-binding bovine S100A1 protein in the apo state (21 kDa) with overall correlation time of 8.1 ns.

Keywords: HNCACB; HN(CO)CACB; Double quantum evolution; Reduced dimensionality; Sequential assignment; Triple resonance; Ubiquitin; S100

1. Introduction

The conventional strategy of protein backbone signal assignment for isotopically enriched proteins is based on triple-resonance three- or four-dimensional experiments [1–4], that utilize ^1J scalar couplings for polarization transfers. These recently reviewed techniques [5,6] enable one to assign all backbone ^1H, ^{13}C, and ^{15}N resonances and to establish sequential connectivities by comparison of experiments which provide intra- and interresidual correlation peaks. The 3D CBCANH, CBCA(CO)NH, and HNCACB techniques [7–10] are especially useful for combined backbone and side-chain sequential assignment purposes, owing to amino acid type specific C_α and C_β chemical shifts and their correlations with the secondary structure.

The transfer experiments $H_{\alpha/\beta} \rightarrow H_N$ employ the constant time evolution of C_α–C_β coherences, thus avoiding modulation due to $^1J(C_\alpha–C_\beta)$ couplings, while in the "out and back" type techniques the resolution is limited by signal splittings due to the evolution of ^{13}C–^{13}C couplings during t_1 period. On the other hand, transfer type sequences are generally less sensitive than out and back variants, because ^{13}C magnetization is affected by transverse relaxation for a longer period, which is necessary to achieve the coherence transfer between the carbon and nitrogen nuclei. For this reason the CBCANH and CBCA(CO)NH experiments are recommended for proteins with slower ^{13}C carbon relaxation [5]. When, however, the ^{13}C transverse relaxation is faster, and/or samples are deuterium enriched, then shorter HNCACB and HN(CO)CACB pulse sequences should be advantageous.

In the present work, we propose a new variant of "out and back" HNCACB and HN(CO)CACB experi-

* Corresponding author. Fax: +48 22 822 59 96.
E-mail address: kozmin@chem.uw.edu.pl (W. Koźmiński).

1090-7807/$ - see front matter © 2004 Elsevier Inc. All rights reserved.
doi:10.1016/j.jmr.2004.08.021

ments, DQ-HN{CACB} and DQ-HN(CO){CACB}, respectively. Curly brackets denote that we observe only one cross peak. corresponding to the sum of $^{13}C_\alpha + {}^{13}C_\beta$ frequencies. These experiments rely on excitation and evolution in t_1, of double quantum (DQ) C_α–C_β coherences, similarly to the original INADEQUATE approach [11]. The spectra could be measured in a 3D manner or, in case of a sufficient resolution, in the 2D reduced dimensionality (RD) [12–15] mode with double quadrature [16–18]. The applicability of the new experiments for the assignment of protein backbone resonances is demonstrated on the samples of ^{13}C, ^{15}N-labeled ubiquitin and 21 kDa ^{13}C, ^{15}N-double labeled Ca^{2+}-binding bovine apo-S100A1. A similar approach of DQ evolution has been already proposed for the DQ-HNCA technique [19]. This technique, however, does not distinguish between intra- and interresidual correlations and thus cannot be used for solving assignment ambiguities.

2. Results and discussion

The pulse sequence schemes for the proposed experiments are depicted in Fig. 1. Both of them employ "out-and-back" coherence transfer with an excitation and detection of H_N protons, and utilize the usual INEPT coherence transfer steps with a constant-time ^{15}N evolution in t_2. In case of sufficient signal dispersion, a 2D RD-type experiment could be acquired by the simultaneous incrementation of t_1 and t_2, while for larger proteins or in less favorable conditions a conventional 3D

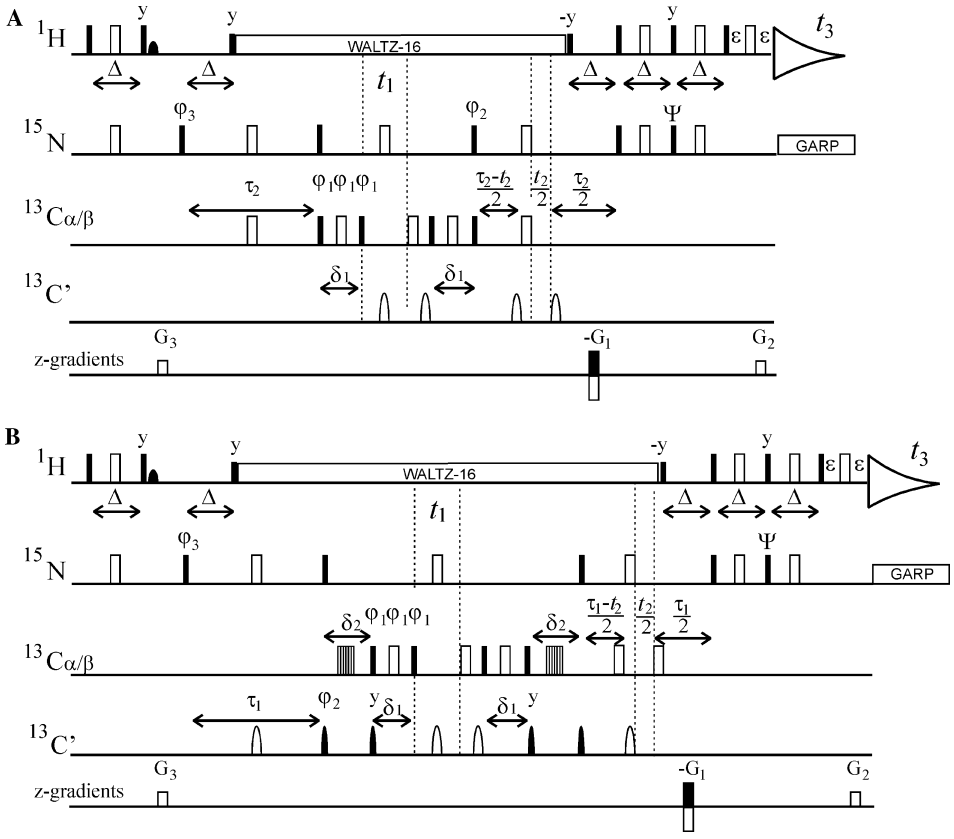

Fig. 1. Pulse sequences for double quantum $C_{\alpha/\beta}$ experiments. (A) DQ-HN{CACB} and (B) DQ-HN(CO){CACB}. Dark-filled and open bars represent π/2 and π pulses, respectively. The selective rectangular pulses were applied on-resonance with γB_1 set to $\Delta\Omega/\sqrt{15}$ and $\Delta\Omega/\sqrt{3}$ for π/2 and π pulses, respectively, where $\Delta\Omega$ is a difference between centers of C′ and $C_{\alpha/\beta}$ spectral regions. Off-resonance selective C′ pulses were realized using linear phase modulated 120.8 μs sinc shapes. The ^{13}C carrier offset was set to the center of $C_{\alpha/\beta}$ region (46 ppm). For the efficient simultaneous inversion of C_α and refocusing of C′ spins the six-element composite pulses [21] were employed. Water flip-back duration of 2.1 ms was applied as a sinc-shaped pulse in the initial INEPT step. All pulses were applied along the rotating-frame x-axis unless indicated otherwise. The delays Δ should be tuned to $0.5/{}^1J(^{15}N, {}^1H)$, τ_1, and τ_2 (28 and 22 ms) were optimized for the maximum amplitude of polarization transfer between C and N, δ_1 and δ_2 were set to 14 and 9 ms, respectively. ε includes the rectangular-shaped gradient pulse and a 100 μs recovery time. The basic phase cycle is: $\varphi_1 = x, y, -x, -y$, $\varphi_2 = 4x, 4(-x)$, $\varphi_3 = 8x, 8(-x)$, and $\varphi_R = 2\varphi_1 + \varphi_2 + \varphi_3$. ^{15}N quadrature was obtained using echo-antiecho PFG-selection by G_1 and G_2 gradients with the duration of 1 ms, and the relative amplitude of $\pm\gamma_H/\gamma_N$. The phase ψ should be set to $-\pi/2$ in echo, and to $+\pi/2$ in antiecho experiments, respectively. The quadrature in the DQ-$C_{\alpha/\beta}$ domain was accomplished by π/4 phase shifts of φ_1. The experiments could be acquired in a 3D mode or in a 2D reduced-dimensionality manner simply by substituting t_2 by κt_1, where κ is a scaling factor. When RD-acquisition is chosen, the double quadrature detection requires acquisition of four data sets per each t_1 increment, i.e., all combinations of φ_1 phases with echo and antiecho, respectively.

acquisition scheme should be preferred. In a 2D RD experiment mode the double quadrature [16] should be applied to enable displaying the F_1 frequencies in all four $\pm\Omega_1$ $\pm\Omega_2$ combinations. The most important modification introduced into proposed pulse sequences, in comparison to their known single-quantum variants, relies on extending the $^{13}C_\alpha$–$^{13}C_\beta$ coupling evolution period to $(2^1J_{CACB})^{-1}$ and retaining the equal phases of three $C_{\alpha\beta}$ pulses directly prior to (φ_1) and after t_1. The four-step cycling of φ_1 rejects all but double-quantum $^{13}C_{\alpha/\beta}$ coherences, which evolve in t_1, and subsequently are converted back to the single-quantum $^{13}C_\alpha$ magnetization. Although it is possible to store separately data sets acquired with φ_1 set to odd and even multiplicities of 90°, and reconstruct zero- and double-quantum spectra by addition and substraction, it would be impossible to obtain quadrature for ZQ-frequencies. Consequently ZQ-spectra would consist both positive and negative ZQ frequencies, i.e., $\pm(\Omega C_\alpha - \Omega C_\beta)$.

The 2D RD spectra, obtained using DQ-HN{CACB} and DQ-HN(CO){CACB} sequences and applied for a 1.5 mM ^{13}C, ^{15}N-labeled ubiquitin sample, are shown in Figs. 2A, B, E, and F, respectively. For comparison the spectra obtained by standard single HNCACB and HN(CO)CACB experiments are plotted, Figs. 2C, D, G, and H, respectively. It is clearly noticeable that the 2-fold reduction of the number of signals facilitates the spectrum analysis and assignment procedures. It is noteworthy that the sum of $^{13}C_\alpha$ and $^{13}C_\beta$ resonance frequencies in proposed DQ-experiments contains useful information about the type of residue of interest, like the standard HNCACB and HN(CO)CACB does. For instance, for serine and threonine residues, whose of $^{13}C_\alpha$ and $^{13}C_\beta$ resonate at high frequencies, the peak appears in the range of 124–140 ppm. Moreover, for threonine and serine residues the situation when the of $^{13}C_\alpha$ resonance lies near the $^{13}C_\beta$ ones take place quite often. In that case, the analysis of DQ-of $^{13}C_{\alpha/\beta}$ spectra results

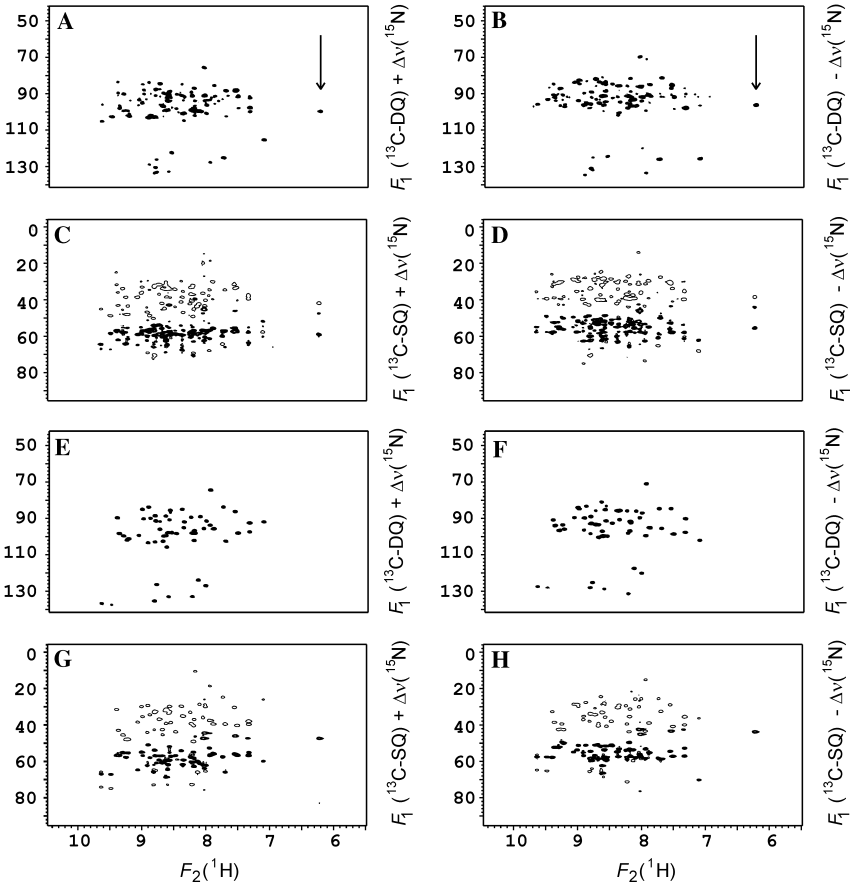

Fig. 2. Contour plots of two-dimensional spectra, obtained using reduced dimensionality 2D DQ-HN{CACB} (A and B) and DQ-HN(CO){CACB} (E and F) sequences from Fig. 1, in comparison with standard, single-quantum, HNCACB (C and D) and HN(CO)CACB (G and H) experiments, applied to a ^{13}C, ^{15}N-labeled ubiquitin sample. Arrows indicate the cross section shown in Fig. 4. For negative signals only one contour level is shown. The time-domain data was processed according to [16], with the retention of positive $^{13}C_{\alpha/\beta}$ DQ and $^{13}C_{\alpha/\beta}$ SQ frequencies. The ^{13}C-DQ scale is given in ppm, thus allowing to obtain the sum of C_α and C_β chemical shifts directly. Thirty-two scans were coherently added for each data set for 128 t_1 increments. The maximum t_1 and t_2 times were 13 and 102 ms, respectively. The spectral width of 10,000 Hz was set for the F_1 dimension in all cases. The relaxation delay of 1.5 s was used. The data matrix containing 128×512 complex points in t_1 and t_2, respectively, was zero-filled to 1024×1024 complex points, a cosine square weighting function was applied prior to the Fourier transformation in both dimensions.

in unwanted effects of accidental cancelation of positive and negative peaks in HNCACB/HN(CO)CACB or peak overlap in CBCA(CO)NH. The other simply identified residue is alanine, which gives a $^{13}C_\alpha + {}^{13}C_\beta$ correlation signal in the range of 64–78 ppm in the DQ-scale. The typical double quantum $^{13}C_\alpha + {}^{13}C_\beta$ spectral regions for different amino acid residues are shown on Fig. 3. A characteristic feature of DQ-$^{13}C_{\alpha/\beta}$ spectra is the lack of signals from $^{13}C_\alpha$ glycine residues whose chemical shifts should be determined using HNCA or/and HN(CO)CA experiments. On Fig. 4 a comparison of the F_1 cross-sections across the amide resonance of Ile36 in spectra from Figs. 2A–F is plotted. In this case, the Gly35 is a preceding residue, so only a single cross-peak is observed in the DQ-HN{CACB} experiment, while it completely vanishes in the DQ-HN(CO){CACB} spectrum.

In standard experiments, with excitation and evolution of SQ-$^{13}C_{\alpha/\beta}$ coherences, delay δ_1 is usually set to $(4^1J_{C\alpha C\beta})^{-1}$ (7.2 ms) to achieve optimal amplitude of both C_α and C_β correlations [5]. Thus, the signal-to-noise ratio is attenuated by the factor of $\sin^2(\pi J\delta_1)$ and is equal to 0.5 for $\delta_1 = 7.2$ ms and $J = 35$ Hz. In proposed DQ-experiments this factor is irrelevant, since the delay δ_1 is extended to $(2^1J_{C\alpha C\beta})^{-1}$ to accomplish a maximum excitation of double-quantum coherences. On the other hand, the excitation of homonuclear DQ-coherences rejects half of the useful signal. Thus, regardless of the relaxation, the sensitivity is retained in DQ-experiments. However, for $T_2(^{13}C)$ of 20 ms the sensitivity loss due to the extension of δ_1 delay could reach even 50%. Although, the $^{13}C_\alpha$–$^{13}C_\beta$ dipolar relaxation disappears for DQ-$^{13}C_{\alpha/\beta}$ coherences, it is replaced by additional, approximately four times stronger, contribution of ^{1}H–^{13}C dipolar relaxation term. Thus, for protonated proteins the relaxation rates of DQ-coherences are expected to be significantly faster. While the $^1J_{C\beta C\gamma}$ couplings similarly affect $^{13}C_\beta$ resonances in SQ- and $^{13}C_{\alpha/\beta}$ DQ-experiments, the advantage of DQ-experiments is clear for longer evolution times owing to the absence of splittings due to active $^1J_{C\alpha C\beta}$ couplings. Moreover, for n $^{13}C_\gamma$ spins, in possible constant-time experiments the optimization of constant evolution delay to $\tau = (^1J_{CC})^{-1}$ would be less critical due to $\cos^n(\pi^1J_{C\beta C\gamma}\tau)$ transfer amplitude in DQ- versus $\cos(\pi^1J_{C\alpha C\beta}\tau)\cos^n(\pi^1J_{C\beta C\gamma}\tau)$ factor, in conventional SQ-experiments. Therefore, DQ-experiments would be especially useful for deuterated proteins with slower relaxing aliphatic carbon nuclei. Similar effect of 2-fold reduction of number of signals could be obtained

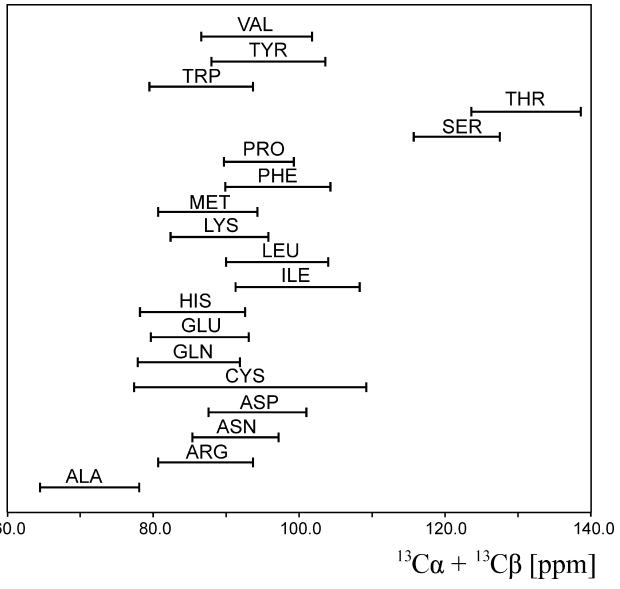

Fig. 3. The typical spectral ranges expected for $^{13}C_\alpha + {}^{13}C_\beta$ DQ frequencies. Data calculated using $^{13}C_\alpha$ and $^{13}C_\beta$ chemical shifts from BioMagnetic Resonance Databank (BMRB http://www.bmrb.wisc.edu/).

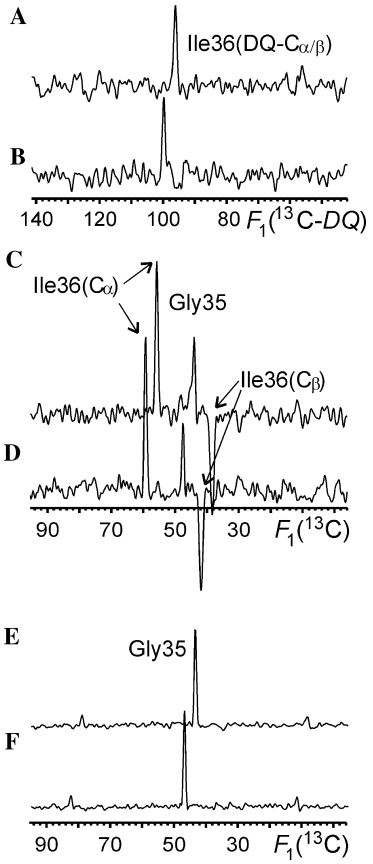

Fig. 4. The comparison of the F_1 cross sections across the amide resonance of Ile36 (preceding residue is Gly35) obtained from the spectra given in Fig. 2. 2D DQ-HN{CACB} (A and B), 2D HNCACB (C and D), and 2D HN(CO)CACB (E and F) experiments. For 2D DQ-HN(CO){CACB} (not shown) no signal was detected. The typical signal-to-noise ratio obtained by HN(CO){CACB} technique for other residues remains in the same relation to SQ variant as obtained using pair DQ-HN{CACB} and HNCACB. The vertical scale is the same for traces (A–D). The spectra are plotted with the retention of positive $^{13}C_{\alpha/\beta}$ SQ and $^{13}C_{\alpha/\beta}$ DQ frequencies. In each pair, in the upper spectrum ^{15}N frequencies are negative in relation to the carrier frequency.

by acquisition of HN(CA)CB and HN(COCA)CB experiments, i.e., by setting δ_1 equal to $(2^1J_{C\alpha C\beta})^{-1}$ for optimum C_α–C_β coherence transfer in conventional single quantum experiments. In such a case signal dispersion would depend on C_β chemical shifts and relaxation loses during δ_1 would be the same as for DQ variants. The effect of C_β–C_γ coupling evolution during t_1 would be observed for all discussed sequences (except alanine residues in DQ-experiments) with the same magnitude.

To test the DQ-HN(CO){CACB} and DQ-HN{CACB} techniques under less favorable conditions, the sample of ^{13}C, ^{15}N-double labeled homodimeric Ca^{2+}-binding bovine apo-S100A1 protein (MM = 21 kDa, $\tau_c = 8.1$ ns) was used. The spectra were collected in a 3D mode. The sample strip plot shown in Fig. 5 clearly demonstrates that the techniques proposed enable one to obtain information about correlations of $H_N(i)$, $N(i)$, $C_{\alpha/\beta}(i)$, and $C_{\alpha/\beta}(i-1)$ resonances.

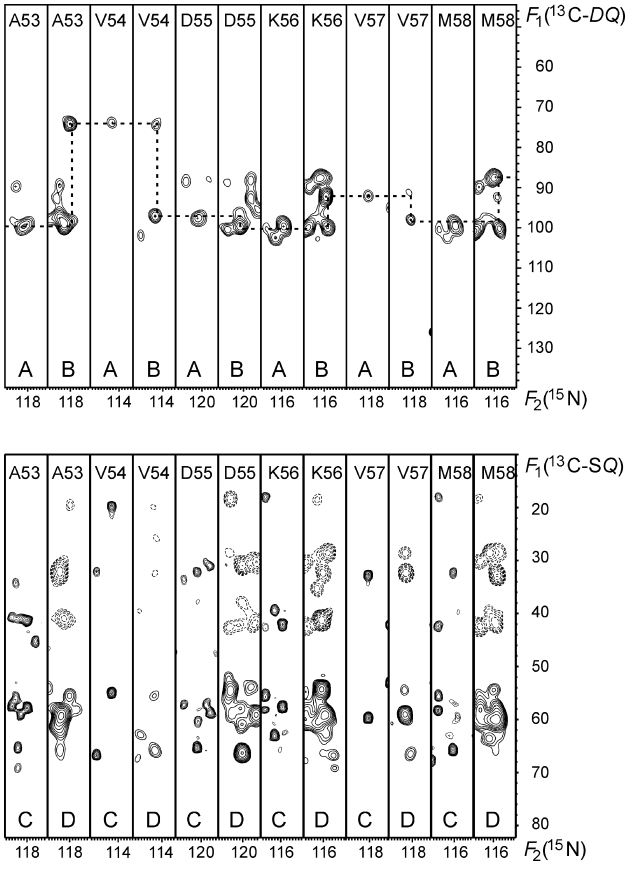

Fig. 5. Strip plots of 3D spectra obtained using DQ-HN(CO){CACB} (A) and DQ-HN{CACB} (B) experiments from Fig. 1, applied to a sample of ^{13}C, ^{15}N-labeled Ca^{2+}-binding bovine apo-S100A1. For comparison the strip plots of 3D CBCA(CO)NH (C) and HNCACB (D) spectra acquired in the same way is given below. The Ala53-Met58 fragment is shown. Sixty-four scans were coherently added for each data set for 32 and 16 increments in t_1 and t_2; acquisition times were 3, 12, and 85 ms in ^{13}C, ^{15}N, and ^1H dimensions, respectively. The spectral width of 12,000 Hz, covering the sum of $^{13}C_\alpha$ and $^{13}C_\beta$ spectral ranges, was set for the ^{13}C dimension. A relaxation delay of 1.4 s was used. The data matrix containing $32 \times 16 \times 512$ complex points in t_1, t_2, and t_3, respectively, was zero-filled to $256 \times 128 \times 1024$ complex points, a cosine square weighting function was applied prior to the Fourier transformation in all dimensions.

The 2D reduced dimensionality spectra were acquired for a sample of 1.5 mM ^{13}C, ^{15}N-labeled ubiquitin in 9:1 H_2O/D_2O at pH 6.0 at 298 K on a Varian Inova 400 spectrometer, while the 3D applications of the techniques proposed were recorded for a sample of 1.1 mM (monomer concentration) ^{13}C, ^{15}N-labeled S100-A1 in 9:1 H_2O/D_2O at pH 6.3 at 308 K on a Varian Unity + 500 spectrometer. Both spectrometers are equipped with Performa II z-PFG units and 5 mm ^1H, ^{13}C, ^{15}N—triple resonance probeheads. High power ^1H, ^{13}C, and ^{15}N $\pi/2$ pulses of 6.7, 14.0, and 44.0 μs, for Inova 400, and of 6.5, 14.2, and 48.0 μs, for Unity + 500, respectively, were employed. The experimental details are given in the figure legends.

3. Conclusions

The pulse sequences proposed employ excitation and evolution of double-quantum $C_{\alpha/\beta}$-coherences. The advantages of these experiments include: a 2-fold reduction of number of correlation peaks and an increased signal dispersion. However, in comparison to conventional variants, the experiments proposed suffer from a sensitivity to fast carbon nuclei relaxation. Therefore, they are expected to be particularly useful for backbone assignment in deuterated proteins. The double quantum evolution could be easily implemented in other variants of $C_{\alpha/\beta}$-type techniques, as for example a sequential HNCACB experiment [20], which would be preferable at high magnetic fields, owing to the omitting of the relay step via $^{13}C'$. The lack of the signal from $^{13}C_\alpha$ carbons for glycine residues does not permit the full sequence-specific backbone assignment procedure based only on DQ-HN{CACB} and DQ-HN(CO){CACB} spectra. However, in our opinion, the application of these techniques simplifies the spectrum analysis, and, in combination with other conventional 3D and/or RD-experiments, may lead to a decrease of the number of spectra needed for the assignment procedure.

Acknowledgments

The authors are grateful to Prof. Andrew R. Byrd (Structural Biophysics Laboratory, National Cancer Institute-Frederick, Frederick, Maryland, USA) for the sample of ^{13}C, ^{15}N-double labeled ubiquitin, and Prof. Andrzej Ejchart (Institute of Biochemistry and Biophysics, Polish Academy of Sciences Warszawa, Poland) for his valuable comments on the manuscript.

References

[1] D. Marion, L.E. Kay, S.W. Sparks, D.A. Torchia, A. Bax, Three-dimensional heteronuclear NMR of ^{15}N labeled proteins, J. Am. Chem. Soc. 111 (1989) 1515–1517.

[2] M. Ikura, L.E. Kay, A. Bax, A novel approach for sequential assignment of ^{1}H, ^{13}C, and ^{15}N spectra of larger proteins: heteronuclear triple-resonance NMR spectroscopy application to calmodulin, Biochemistry 29 (1990) 4659–4667.

[3] A. Bax, S. Grzesiek, Methodological advances in protein NMR, Acc. Chem. Res. 26 (1993) 131–138.

[4] T. Yamazaki, W. Lee, C.H. Arrowsmith, D.R. Muhandiram, L.E. Kay, A suite of triple resonance NMR experiments for the backbone assignment of ^{15}N, ^{13}C, ^{2}H labeled proteins with high sensitivity, J. Am. Chem. Soc. 116 (1994) 11655–11666.

[5] M. Sattler, J. Schleuchter, C. Griesinger, Heteronuclear multidimensional NMR experiments for the structure determination of proteins in solution employing pulsed field gradients, Prog. NMR Spectrosc. 34 (1999) 93–158.

[6] P. Permi, A. Annila, Coherence transfer in proteins, Prog. NMR Spectrosc. 44 (2004) 97–137.

[7] S. Grzesiek, A. Bax, Correlating backbone amide and sidechain resonances in larger proteins by multiple relayed triple resonance NMR, J. Am. Chem. Soc. 114 (1992) 6291–6293.

[8] S. Grzesiek, A. Bax, An efficient experiment for sequential backbone assignment of medium sized isotopically enriched proteins, J. Magn. Reson. 99 (1992) 201–207.

[9] S. Grzesiek, A. Bax, Amino acid type determination in the sequential assignment procedure of uniformly ^{13}C/^{15}N enriched proteins, J. Biomol. NMR 3 (1993) 185–204.

[10] M. Wittekind, I. Müller, HNCACB, a high-sensitivity 3D NMR experiment to correlate amide-proton and nitrogen resonances with the alpha- and beta-carbon resonances in proteins, J. Magn. Reson. B 101 (1993) 201–205.

[11] A. Bax, T.A. Frenkiel, R. Freeman, A NMR technique for tracing out the carbon skeleton of an organic molecule, J. Am. Chem. Soc. 103 (1981) 2102–2104.

[12] T. Szyperski, G. Wider, J.H. Buschweller, K. Wüthrich, Reduced dimensionality in triple-resonance NMR experiments, J. Am. Chem. Soc. 115 (1993) 9307–9308.

[13] B. Brutscher, J.P. Simorre, M.S. Caffrey, D. Marion, Design of a complete set of two-dimensional triple-resonance experiments for assigning labeled proteins, J. Magn. Reson. B 105 (1994) 77–82.

[14] F. Löhr, H. Rüterjans, A new triple-resonance experiment for the sequential assignment of bacbone resonances in proteins, J. Biomol. NMR 6 (1995) 189–197.

[15] K. Ding, A.M. Gronenborn, Novel 2D triple-resonance NMR experiments for sequential resonance assignments of proteins, J. Magn. Reson. 156 (2002) 262–268.

[16] W. Koźminski, I. Zhukov, Multiple quadrature detection in reduced dimensionality experiments, J. Biomol. NMR 26 (2003) 157–166.

[17] S. Kim, T. Szyperski, GFT NMR, a new approach to rapidly obtain precise high-dimensional NMR spectral information, J. Am. Chem. Soc. 125 (2003) 1385–1393.

[18] B. Bersch, E. Rossy, J. Coves, B. Brutscher, Optimized set of two-dimensional experiments for fast sequential assignment, secondary structure determination, and backbone fold validation of ^{13}C/^{15}N-labelled proteins, J Biomol. NMR 27 (2003) 57–67.

[19] D. Nietlispach, Y. Ito, E.D. Laue, A novel approach for the sequential backbone assignment of larger proteins: selective intra-HNCA and DQ-HNCA, J. Am. Chem. Soc. 124 (2002) 11199–11207.

[20] A. Meissner, O.W. Sørensen, Sequential HNCACB and CBCANH protein NMR pulse sequences, J. Magn. Reson. 151 (2001) 328–331.

[21] A.J. Shaka, Composite pulses for ultra-broadband spin inversion, Chem. Phys. Lett. 120 (1985) 201–205.